Structural and magnetic isomers of $M(BN)_{36}$ and $M_4(BN)_{36}$ clusters (M=Ti,V,Cr,Mn,Fe,Co,Ni,Cu): An *ab initio* density functional study

Sandeep Nigam, S. K. Kulshreshtha, and Chiranjib Majumder*
Chemistry Division, Bhabha Atomic Research Centre, Mumbai 400085, India
(Received 2 November 2007; published 29 February 2008)

Using the plane wave based pseudopotential method under the density functional formalism, the geometry and electronic structures of M and M_4 encaged $(BN)_{36}$ clusters have been investigated, where M represents Ti, V, Cr, Mn, Fe, Co, Ni, and Cu atoms. The lowest energy structure of the $M(BN)_{36}$ cluster shows that the impurity atom prefers to occupy either the center or off-center and close to the hexagonal ring of the cage. Geometry and electronic structures of M_4 clusters have been calculated in the bare state as well as inside the octahedral $(BN)_{36}$ cluster. For free M_4 clusters, except Cu_4, which forms a planar rhombus structure, all other tetramer clusters adopt three dimensional bent rhombus or tetrahedron configuration. In sharp contrast, the equilibrium structure of M_4 clusters inside the $(BN)_{36}$ cage results in significant deformation in comparison to that in the free state. Unlike others, it is found that the stability of V_4, Fe_4, Co_4, and Ni_4 tetramers have been enhanced inside the cage. Importantly, these small clusters are found to retain their magnetic nature even after encaging them inside the $(BN)_{36}$ cluster. In general, the magnetic moment of the M_4 clusters are found to decrease inside the $(BN)_{36}$ cage, except that for Cr_4 cluster, which showed significant increase in the magnetic moment. The electronic density of state analysis of these systems shows additional electronic states in the large gap of $(BN)_{36}$ cluster originated by the M atoms or M_4 clusters.

DOI: 10.1103/PhysRevB.77.075438 PACS number(s): 73.22.−f, 36.40.Cg, 36.40.Qv, 36.40.Ei

I. INTRODUCTION

Small clusters of transition metal elements show higher magnetic moments than the corresponding bulk solids. The increase in magnetic moment is largely due to surface sites that have lower coordination number than the atoms present in the interior or bulk.[1] These magnetic materials have important applications in nanoelectronic devices, magnetic recording media, and biological sensors. However, oxidation and wear resistance of the surface become a problem for naked clusters. Therefore, encaging of these magnetic clusters inside an insulator will have significant advantage for their use in industrial or medicinal applications.[2]

Boron nitride (BN) is a good insulating material (band gap of ~5.5 eV) with excellent chemical and thermal stability. It may therefore serve as an insulating and protective shield for encapsulating magnetic particles and prevent the degradation of magnetic particles from oxidation and chemical modifications. Recently, BN based nanomaterials, such as clusters, nanocapsules, nanohorns, and nanotubes, had been discovered and studied for their chemical and electronic stability.[3–25] In a series of experiments, Oku and co-workers have reported the synthesis of boron nitride clusters of different sizes.[4–15] Perhaps the most interesting result of their work was the production of $(BN)_{24}$ in abundance. Other than this, $(BN)_{36}$ cluster was observed on and inside the BN nanotubes, and their sizes were in the range of 0.7–1.0 nm.[7] In another set of experiments, Stephan *et al.* irradiated BN (Ref. 16) and observed small BN cagelike molecules. The products after irradiation were either closed packed or nested cages and most cages had the diameter in the size range of 4–7 Å. The octahedral motif was proposed as the most probable structures for $(BN)_{12}$, $(BN)_{16}$, and $(BN)_{28}$ cages. Subsequently, Goldberg *et al.* corroborated the proposal of octahedral structures for the observed BN cages[17] using the electron microscope. From the high-resolution transmission electron microscopy images, they observed single-shelled cages with size of 8–10 Å, with rectanglelike outlines for $(BN)_{36}$ cluster as proposed by Oku *et al.*[5] and Alexandre *et al.*[18]

The presence of impurity metal atoms or clusters inside the nanocage or nanotubes during their synthesis can significantly modify the physicochemical properties. In order to understand this effect, many experimental and theoretical studies have been reported on the metal encapsulated BN nanomaterial.[5,16,19–25] Bando *et al.* prepared BN nanotubes filled with Fe-Ni alloy nanorods.[20] Tang *et al.* have reported the *in situ* filling of BN nanotubes with cubic Ni metal and $NiSi_2$ nanowires followed by electron microscopic study of the resultant structures.[21] Han *et al.* demonstrated the encapsulation of various potassium halides (KCl, KBr, and KI) in BN nanotubes.[22] Xu *et al.* have reported the transmission electron microscopy study of BN nanotubes filled with cobalt. In fact, they have reported that the transition metals, Fe, Co, and Ni, are the most effective catalysts for the formation of BN nanotubes.[23] Peng *et al.* have made a comparative study on the structural, energetic, and magnetic properties of $B_xC_yN_z$ composite single-walled nanotubes filled with transition-metal nanowires using first-principles calculations.[24] They found that interaction between the nanotube and nanowire weakens the magnetism of the nanowire.[24] Koia *et al.* produced Fe-filled BN nanotubes and investigated them by high-resolution electron microscopy, high-angle annular dark-field scanning transmission electron microscopy, electron diffraction, and energy dispersive x-ray spectroscopy.[12] They have also reported the synthesis of BN nanocapsules encaging Fe and Co nanoparticles.[13] In another work, Oku and co-workers have studied the $Fe/La/Y(BN)_{36}$ cluster by high-resolution electron microscopy.[14] Recently, Batista *et al.* have carried out first-principles calculation on

FIG. 1. Ground state atomic configuration of the $(BN)_{36}$ cluster. The gray and black circles represents boron and nitrogen atoms, respectively.

transition metal (Fe, Co, and W) doped $(BN)_{36}$ fullerene and they found that these metal atoms does not induce magnetic moment on the BN cage.[25]

In the present work, we have investigated the atomic, magnetic, and electronic structures of $M(BN)_{36}$ and $M_4(BN)_{36}$ clusters, where M represents Ti, V, Cr, Mn, Fe, Co, Ni, and Cu atoms. The major objective of this study is threefold: (i) To find out the equilibrium structure of $M(BN)_{36}$ and $M_4(BN)_{36}$ clusters. (ii) What is the difference in the ground state structure of M_4 clusters inside and outside the cage of $(BN)_{36}$ cluster? (iii) Whether small metal clusters can retain their magnetic properties even after encaging inside the $(BN)_{36}$ nanocluster. The choice of tetramer clusters was governed by the fact that these are the smallest clusters, which can have either planar or nonplanar atomic structure in the ground state.

II. COMPUTATIONAL DETAILS

The total energy calculation and geometry optimization of several isomeric structure of M_4, $M(BN)_{36}$, and $M_4(BN)_{36}$ (M=Ti, V, Cr, Mn, Fe, Co, Ni, and Cu) clusters were performed under density functional theory formalism and plane-wave basis set as implemented in the Vienna *ab initio* simulation package (VASP).[26] The electron-ion interaction was described by the full-potential all-electron projector augmented wave (PAW) method,[27] as implemented in VASP by Kresse and Joubert.[28] The PAW pseudopotential was generated taking scalar relativistic corrections into account. The spin-polarized generalized gradient approximation[29] has been used to calculate the exchange-correlation energy. The cutoff energy for the plane-wave basis set was fixed at 400 eV for all calculations performed in this study. A simple cubic supercell of side 15 Å was used to ensure that the periodically repeated cluster images do not interact with each other. The Brillouin zone integrations are carried out at the Γ point only. The geometry of the clusters has been determined by ionic relaxation using a conjugate gradient minimization and the exact Hellmann-Feynman forces. The geometries are considered to be converged when the force on each ion becomes 0.01 eV/Å or less. The total energy convergence was tested with respect to the plane-wave basis set size and simulation cell size, and the total energy was found to be accurate to with in 1 meV. In order to check the effect of relativistic corrections, total energy calculations were carried out after incorporating the spin-orbit coupling effect. However, no significant changes were found on the binding energies of these clusters.

A fixed magnetic moment calculation on a series of magnetic isomers yields important information on magnetostructural effects. In order to obtain the information on the magnetic isomers, we have used the fixed moment mode[30] where the total magnetic moment of the cluster was constrained to a fixed value by fixing the occupation numbers of the spin-up and spin-down channels. The local magnetic moments were

TABLE I. Equilibrium position of impurity atom, magnetic moment, and interaction energy (interaction energy (Int. En) $=E[M(BN)_{36}]_{opt}-E[(BN)_{36}]_{opt}-E(M)$.) (Int. En.) of low lying isomers [for Cr, Mn, and Cu atoms only two isomers (center and tetragonal) were found to be stable] of $M(BN)_{36}$ cluster.

M	Position	μ_B	Int. En. (eV)
Ti	Hexagonal	4	−1.02
	Tetragonal	0	−0.29
	Center	4	−0.15
V	Hexagonal	5	−0.40
	Center	5	−0.18
	Tetragonal	1	0.28
Cr	Center	6	−0.06
	Tetragonal	2	2.34
Mn	Center	5	0.10
	Tetragonal	3	1.72
Fe	Hexagonal	4	−0.20
	Center	4	−0.07
	Tetragonal	2	0.65
Co	Hexagonal	3	−0.64
	Center	3	−0.10
	Tetragonal	1	0.28
Ni	Hexagonal	0	−0.78
	Tetragonal	0	−0.48
	Center	2	−0.28
Cu	Center	1	−0.12
	Tetragonal	1	−0.10

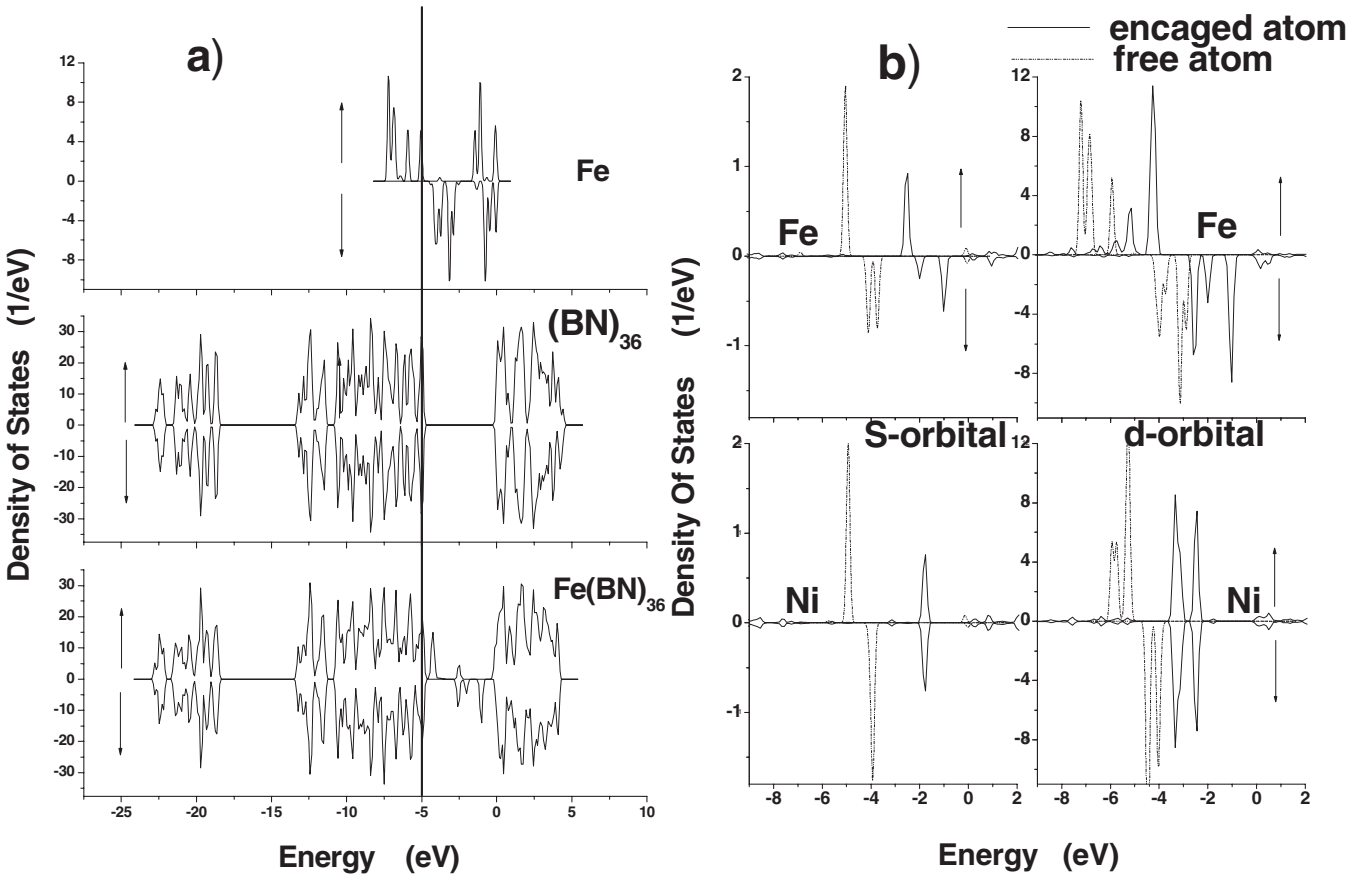

FIG. 2. (a) The total density of states of the Fe atom, $(BN)_{36}$ cluster, and $Fe(BN)_{36}$ clusters. The up and down arrows represents the alpha and beta spins, respectively. The vertical line indicates the position of the HOMO energy level for the $(BN)_{36}$ cluster. (b) The fragmented density of states of Fe and Ni atoms in free and encaged states.

obtained by projecting the plane wave into angular momentum components of all occupied eigenstates onto spherical waves within slightly overlapping atomic spheres and integrating the resulting spin-polarized local densities of state. The radius of the spheres has been chosen such as to reproduce the correct total moment. However, this decomposition is only representative and is expected to give a qualitative character of each state.

III. RESULTS AND DISCUSSION

In order to understand the geometrical and electronic changes that occur by the presence of M atoms or M_4 clusters inside $(BN)_{36}$, we have systematically calculated the geometries of $(BN)_{36}$, $M(BN)_{36}$, M_4, and $M_4(BN)_{36}$ clusters, respectively. In the following section we present our results in the above mentioned sequence.

A. Geometries and stabilities of $(BN)_{36}$ and $M(BN)_{36}$ clusters

The ground state atomic configuration of the $(BN)_{36}$ cluster is depicted in Fig. 1, which favors cagelike geometry formed by six squares and 32 hexagonal rings. The B-N distance in the four member ring is found to be 1.47 Å, which elongates up to 1.49 Å in the hexagonal ring. The internal diameter of this cage is estimated to be 7.97 Å, which is slightly more than the C_{60} cage. The average binding energy of $(BN)_{36}$ cluster is calculated to be 8.43 eV/atom, which after correcting with respect to the spin-polarized atom energy is found to be 6.76 eV/atom (average binding energy=$[E(BN)_{36}$-$E(B)$-$E(N)]/72$). The higher stability of this cage cluster is further corroborated by its large energy gap of 4.95 eV observed between the highest occupied molecular orbital and lowest unoccupied molecular orbital (HOMO-LUMO) energy levels. These results were compared with previous reports and found to be in good agreement.[15,31,32]

The equilibrium geometry of the M atom encapsulated $(BN)_{36}$ clusters was obtained by optimizing four initial guess structures: (i) the M atom occupying the center position of the cage, (ii) the M atom is placed off center and close to the tetragonal ring, (iii) the M atom is placed off-center and close to the hexagonal ring, and (iv) the M atom is connected to the bridge site of the tetragonal and hexagonal ring. After geometry optimization, a comparison of total energies between different isomers shows, while few M atoms (Ti, V, Fe, Co, and Ni) favor to occupy an off-center position close to the hexagonal ring others remain at the center (Cr, Mn, and Cu) due to very weak interaction with the cage. The results are summarized in Table I by enlisting the interaction energy and magnetic moment for the lower energy isomers

TABLE II. Magnetic moment and interatomic separation (IS) of M_2 dimers along with its experimental values (expt.) are taken from Ref. 33.

M_2	μ_B	IS (Å)	IS (Å) (expt.)
Ti	2	1.90	1.94
V	2	1.74	1.77
Cr	0	1.52	1.68
Mn	10	2.59	~3.4
Fe	6	1.98	2.02
Co	4	1.96	
Ni	2	2.08	2.15
Cu	0	2.22	2.21

that has been calculated in this work. In this context, it should be mentioned that in another recent study, Batista *et al.*[25] have reported the interactions of Fe and Co atoms with $(BN)_{36}$ cage, where impurity atoms were found to occupy the tetragonal and bridge sites from outside the cage. In another study, Oku and co-workers [14] carried out semiempirical calculations on endohedral $Fe(BN)_{36}$ cluster and found that the doping element attaches to one of the hexagonal ring resulting in expansion of host cluster.

It is clear from this table that when metal atoms are placed close to the hexagonal ring, the interaction is stronger than that placed at the center. From the geometrical point of view, the presence of metal atoms inside the $(BN)_{36}$ cage has very negligible effect on the cage structure. So also in the case of electronic structure, except that for Ni, for which the atomic moment of Ni is quenched and the $Ni(BN)_{36}$ cluster shows singlet spin state. Apart from it, all elements follow the trend of their respective atomic moments in the gas phase. Moreover, the details of the eigenvalue spectrum of these clusters suggest that impurity atoms introduces their energy states in the large gap between the HOMO-LUMO energy levels of the $(BN)_{36}$ cage, which is consistence with previous observations.[25] This feature has been illustrated in Fig. 2 by considering two representative cases as $Fe(BN)_{36}$ and $Ni(BN)_{36}$ clusters. It is found that while in case of Fe atom, the spins are polarized even after encapsulating it, for Ni, the spin moments are completely quenched, thereby resulting in singlet spin multiplicity for the $Ni(BN)_{36}$ cluster.

B. Geometries and stabilities of M_4 and $M_4(BN)_{36}$ clusters

Before proceeding to calculate the ground state geometries and energetics of M_4 clusters of transition metal elements, test calculations were performed for M_2 systems to understand the interactions between M atoms. The results are summarized in Table II. A comparison between these results and experiment values[33] shows good agreement, which provide confidence of the computational method adopted in this work.

The stable low-lying isomers of free M_4 clusters was calculated by optimizing different configurations starting from a planar to compact tetrahedron structures. It is found that depending on the nature of the interatomic forces, M_4 clusters adopt (a) planar rhombus, (b) bent rhombus (BR), and (c) tetrahedral structure. The typical geometrical representations are shown in Fig. 3. The geometrical transformation from the planar rhombus to three dimensional compact tetrahedron has been analyzed in terms of the dihedral angle (DA) of atom 3 (viz., Fig. 3) with respect to the plane formed by 1, 2, and 4. The diagonal distances (2-4) and (1-3) have also been taken into account to visualize the closing and opening of the geometry. Details of the geometrical parameters, binding energy, and magnetic moment values are listed in Table III for all M_4 clusters.

Once the geometries of the $(BN)_{36}$ cage and M_4 clusters are established, it is of interest to study the structural and electronic properties of $M_4(BN)_{36}$ cluster. In particular, it is important to investigate the stability and structural evolution of tetramer when the M atoms agglomerate inside the cage and compare these results with previously calculated M_4 clusters in the free state. For this purpose, we have carried out a series of geometry optimizations of M_4 clusters placed at the center of $(BN)_{36}$ cage, as shown in Fig. 4. To get the lowest energy isomer of the M_4 cluster inside $(BN)_{36}$ cage, three different isomers of M_4 clusters [(a) planar rhombus, (b) bent rhombus, and (c) tetrahedral (shown in Fig. 3)] were used as the starting configurations. The geometry optimization of the whole $M_4(BN)_{36}$ system was carried out without any symmetry constraint. The results are summarized in Table IV giving the details of the interatomic separations and bond angles for the bare and caged clusters. In the following sections, we have systematically discussed the comparative analysis of the M_4 and $M_4(BN)_{36}$ cluster separately.

The equilibrium geometry of the Ti_4 cluster is reported by several workers. Using the density functional theory (DFT)–local spin density approximation method,[35] Wei *et al.* have

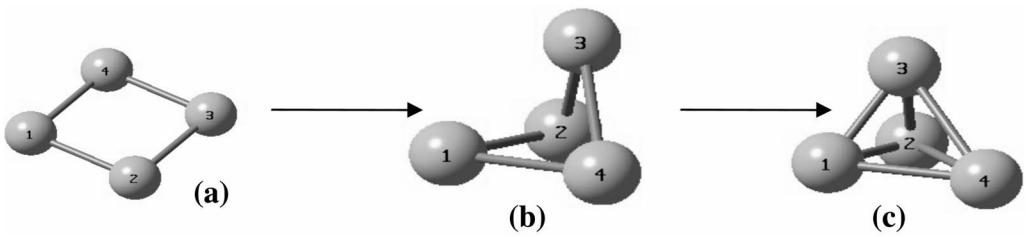

FIG. 3. Three different geometries that represent the ground state atomic configurations of M_4 clusters: (a) planar rhombus, (b) bent rhombus, and (c) tetrahedral.

TABLE III. Geometry, energetics, and magnetic moments of free M_4 clusters. Bulk cohesive energy values for these metals have been taken from Ref. 34.

Cluster	Optimized geometry	Magnetic moment (μ_B)	BE/atom (eV)	Bulk cohesive energy (eV)
Ti_4	Dis. T_d	4	−2.60	4.67
V_4	T_d	0	−2.38	5.11
Cr_4	BR	0	−1.28	3.94
Mn_4	T_d	20	−1.18	2.79
Fe_4	Dis. T_d	14	−2.13	4.14
Co_4	BR	10	−2.27	4.23
Ni_4	Dis. T_d	4	−2.26	4.28
Cu_4	Planar D_{2h}	0	−1.58	3.37

found a capped triangle (C_{3v} symmetry) as the lowest energy structure. Followed by this, Zhao *et al.*[36] have obtained a regular tetrahedron using the ultrasoft nonlocal pseudopotentials. In another work by Castro *et al.*,[37] distorted tetrahedron was reported to be the lowest energy isomer. In good agreement with this work, we found a distorted tetrahedron (more compressed than regular T_d with dihedral angle of 65°) with magnetic moment of $4\mu_B$. The distances between the Ti atoms are found to be 2.51 (1-2, 1-4, 2-3, and 3-4) and 2.38 Å (1-3 and 2-4). The binding energy of the Ti_4 cluster is estimated to be 2.60 eV/atom. The compact tetrahedron structure with lower magnetic moment ($2\mu_B$) is found to be 0.23 eV higher in energy. When the geometry of the Ti_4 cluster was optimized inside the $(BN)_{36}$ cage, starting with possible isomeric forms of Ti_4 cluster, the lowest energy conformation of the Ti_4 cluster is found to adopt the trigonal pyramidal structure (symmetry C_{3v}). It may be noted that this is different than its lowest energy isomer in the free state, which forms distorted tetrahedron. The elongation in the interatomic separations between Ti atoms results in an increase of the dihedral angle from 65° to 68°. The Ti-Ti separations in the base plane of the equilateral triangle are 2.71 Å and the distance between the capping atom and the base atoms is 2.45 Å. For the $Ti_4(BN)_{36}$ cluster, the Ti-B and Ti-N distances are found to be 2.36 and 2.24 Å, respectively. The magnetic moment of the Ti_4 cluster inside the cage is reduced from $4\mu_B$ to $2\mu_B$. The next higher energy isomer of Ti_4, which form a bent rhombus configuration (DA=83°) with a magnetic moment of $4\mu_B$ is 0.30 eV higher in energy with respect to the C_{3v} isomer. Another isomer with similar structural configuration (DA=80°) but having the magnetic moment of $6\mu_B$ shows 0.51 eV higher in the energy. Here, it should be noted that the isomer with C_{3v} symmetry is not an equilibrium structure in the free state. The average binding energy (average binding energy inside the cage (BE) $=\{E[M_4(BN)_{36}]_{opt}-E[(BN)_{36}]_{opt}-4E(M)\}/4$) of the Ti_4 cluster inside the cage is estimated to be 2.51 eV/atom.

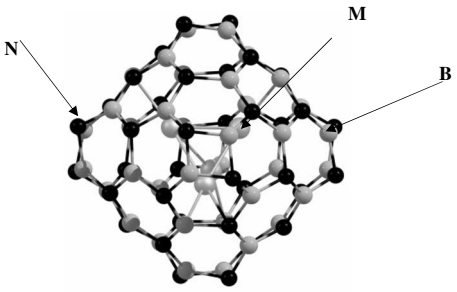

FIG. 4. Representative atomic configuration of the M_4 clusters inside the $(BN)_{36}$ cluster.

The equilibrium structure of V_4 cluster has been predicted previously[38–40] using different methodologies. While Gronbeck and Rosen have found planar structure of V_4 based on the linear combination of atomic orbital (LCAO) approach,[38] Wu and Ray have carried out an all electron calculation and obtained regular tetrahedral geometry with zero magnetic moment.[39] Recently, Li *et al.*, using a real-space pseudopotential method, have found V_4 as rhombus.[40] In the present work, we show that V_4 favors a regular tetrahedron as the lowest energy isomer with zero magnetic moment. The bond distance among the vanadium atoms is estimated to be 2.22 Å and the DA is 70.54°. The average binding energy of the V_4 cluster is found to be 2.38 eV/atom. The optimization of the V_4 cluster inside the (BN) cage leads to very small change (about 0.04–0.06 Å) in comparison to its ground state geometry outside. For $V_4(BN)_{36}$, the smallest V-B and V-N distances are found to be 2.32 and 2.22 Å, respectively. Another isomer of bent rhombus configuration (DA=83° and a magnetic moment of $2\mu_B$) was found to be 0.31 eV higher in energy than the T_d isomer. So unlike Ti_4, V_4 cluster favors similar atomic configuration inside and outside the cage of $(BN)_{36}$ cluster. The average binding energy calculated for V_4 cluster inside the cage is found to be 2.49 eV/atom. Thus, it is clear that the stability of the V_4 cluster is enhanced inside the cage of $(BN)_{36}$ cluster.

The geometry optimization of the Cr_4 clusters attracts some special attention as it is formed by two extraordinary stable Cr_2 fragments.[41] Cheng and Wang have found the higher symmetry D_{2h} planar rhombus as the lowest energy isomer for Cr_4 cluster.[41] In another study, Hobbs *et al.* have reported a tetrahedron structure for Cr_4.[42]. Wang *et al.*[43] have investigated magnetic chromium clusters at the DFT/BPW91 level, taking all electron into account, and obtained a bent rhombus structure having two short and two long bond lengths with D_2 symmetry as a lowest energy structure of Cr_4. A similar structure was also found in our present study. The short bond length of bent rhombus is 1.64 Å which is only 0.12 Å larger than the bond length of chromium dimer. The larger side of rhombus is 2.72 Å which reflect very poor interaction between two Cr atoms. The dihedral angle is found to be 113.05° for this structure. The binding energy of this Cr_4 cluster is estimated to be 1.28 eV/atom.The geometry optimization of the $Cr_4(BN)_{36}$ cluster was carried out starting with different initial geometries that were found for Cr_4 cluster inside the cage. The relaxation of the Cr_4 isomer inside the cage showed significant geometrical transformation, where the slightly bent rhombus (DA=113°) optimizes into a more compact structure by reducing the DA up to 83°.

TABLE IV. Comparison of the interatomic distances between metal atoms, bond angle and dihedral angle (DA) of M_4 cluster in free and encapsulated states numbers presented in parentheses correspond to the encaged clusters.

M_4	1-2 (Å)	1-4 (Å)	2-3 (Å)	3-4 (Å)	1-3 (Å)	2-4 (Å)	Angle ∠412	Angle ∠432	Angle ∠123	Angle ∠143	DA 124/3
Ti	2.51 (2.70)	2.51 (2.45)	2.51 (2.71)	2.51 (2.45)	2.38 (2.71)	2.38 (2.45)	56.54 (60.22)	56.54 (67.13)	56.54 (56.69)	56.54 (56.46)	65.01 (67.70)
V	2.22 (2.31)	2.22 (2.29)	2.22 (2.26)	2.22 (2.23)	2.22 (2.26)	2.22 (2.28)	60 (59.59)	60 (61.22)	60 (59.28)	60 (60.12)	70.54 (70.45)
Cr	2.72 (2.31)	1.64 (2.58)	1.64 (1.90)	2.72 (2.72)	2.96 (2.84)	2.96 (2.25)	81.23 (65.82)	81.08 (62.92)	81.34 (71.1)	81.34 (66.6)	113.05 (82.99)
Mn	2.70 (2.47)	2.70 (2.47)	2.70 (2.35)	2.70 (2.35)	2.70 (2.35)	2.70 (2.47)	60 (60)	60 (63.55)	60 (58.22)	60 (58.24)	70.75 (69.06)
Fe	2.24 (2.32)	2.24 (2.25)	2.24 (2.34)	2.24 (2.39)	2.53 (2.30)	2.53 (2.25)	69 (59)	69 (56.8)	69 (59.18)	69 (59.34)	86.6 (74.76)
Co	2.14 (2.44)	2.14 (2.31)	2.14 (2.21)	2.14 (2.17)	2.72 (2.30)	2.72 (2.44)	79 (59.13)	79 (59.13)	79 (59.88)	79 (59.31)	110.93 (68.78)
Ni	2.31 (2.33)	2.31 (2.33)	2.31 (2.28)	2.31 (2.36)	2.21 (2.44)	2.21 (2.35)	57 (60.52)	57 (60.77)	57 (63.76)	57 (62.64)	73 (74.73)
Cu	2.38 (2.31)	2.38 (2.33)	2.38 (2.33)	2.38 (2.31)	2.27 (2.35)	4.17 (2.77)	123 (73.01)	123 (73.45)	57 (60.48)	57 (60.83)	180 (78.05)

The smallest Cr-B and Cr-N distances are 2.27 and 2.21 Å, respectively. The structural changes were derived by the reduction of the diagonal bond to facilitate the packing of the geometry. As the Cr_4 cluster modifies its geometry inside the cage, so also its electronic and magnetic structures. The magnetic moment of the Cr_4 cluster inside the $(BN)_{36}$ cage is found to be enhanced up to $8\mu_B$. The average binding energy of the Cr_4 cluster inside the cage is estimated to be only 0.76 eV/atom. The reduction in the stability of Cr_4 inside the cage can be attributed to the significant stain created by the bending of the rhombus structure, which is more stable in the free state.

Previous calculations by Pederson *et al.*[44] and Bobadova-Parvanova *et al.*[45] have predicted regular tetrahedron structure of Mn_4 cluster with large magnetic moment of $20\mu_B$. In the present study, we find a regular tetrahedron structure (2.70 Å bond length and DA=70.75°) as the lowest energy isomer for Mn_4 cluster, which is in line with the previous results. The total magnetic moment is estimated to be $20\mu_B$ which is distributed homogeneously over all the atoms. The average binding energy of this Mn_4 cluster is calculated to be 1.22 eV/atom. Another isomer, with C_{3v} symmetry where an atom is capping the equilateral triangle, was found 0.07 eV higher in energy. The C_{3v} isomer has its base as an equilateral triangle with 2.67 Å as the interatomic separation between the base atoms and the capping atom is 2.51 Å away from each of the atoms of base triangle. The optimization of the Mn_4 inside $(BN)_{36}$ shows that it prefers capped triangle (C_{3v} symmetry) rather than a regular tetrahedron. The equilateral triangle is formed with 2.45 Å as the interatomic separation between the base atoms and the capped atom is 2.34 Å away from each of the atoms of the triangle, but the dihedral angle of capping atom (atom 3) from the plane of triangle remains same. The smallest Mn-B and Mn-N distances are found to be 2.27 and 2.17 Å, respectively, for the $Mn_4(BN)_{36}$ cluster. The total moment of the Mn_4 cluster inside the cage is found to be reduced from $20\mu_B$ to $10\mu_B$, which can be attributed to the changes, occurred in the geometrical parameters of the Mn_4 cluster. Further calculations were carried out by fixing the magnetic moment at $14\mu_B$, $16\mu_B$, $20\mu_B$ which resulted in 0.51, 1.97, and 4.27 eV, respectively, in comparison to that of the lowest energy isomer. The average binding energy of the Mn_4 cluster inside the cage is estimated to be only 1.04 eV/atom.

The ground state geometry of the Fe_4 cluster has been reported by several groups. It is found that Fe_4 cluster favors a regular or slightly distorted tetrahedron, depending on the theoretical methods adopted[42] [local density approximation (LDA) or generalized gradient approximation (GGA)]. The results showed that Fe_4 favors distorted tetrahedron structure under both these schemes but there is a difference in magnetic structure at these two levels. While LDA predicts total magnetic moment of the Fe_4 cluster as $12\mu_B$, GGA gives higher value of $14\mu_B$.[42] In another study, using the LCAO approach, Chen *et al.*[46] have found Fe_4 as a regular tetrahedron structure with $12\mu_B$ magnetic moment. Jones *et al.*[47] have found Fe_4 as a distorted tetrahedron (2.19 Å, 2.38 Å, BE=2.11 eV/atom) with a magnetic moment value of $14\mu_B$. In overall agreement with previously reported results,[42] we have obtained a distorted tetrahedron (DA=87°) as the lowest energy isomer of Fe_4 with total moment of $14\mu_B$. The interatomic separations are found to vary from 2.24 to 2.54 Å (Table IV). The binding energy of this Fe_4 cluster is estimated to be 2.13 eV/atom. The next higher energy isomer having the total magnetic moment of $12\mu_B$ and the distorted tetrahedron structure is 0.14 eV higher in energy. The optimization of caged Fe_4 cluster was made considering the three different geometries inside the $(BN)_{36}$ cage using the same method. The results show that the distorted tetrahedron structure of Fe_4 structure becomes more compact by reducing the DA from 87° to 75° and the corresponding diagonal distances decrease from 2.54 to 2.30 Å. The clos-

ing of the geometry inside the cage results in quenching of the magnetic moments of Fe_4 cluster from $14\mu_B$ to $10\mu_B$. For the encapsulated $Fe_4(BN)_{36}$ cluster, the Fe-B and Fe-N distances are found to be 2.02 and 2.25 Å, respectively. We have also attempted to optimize the $Fe_4(BN)_{36}$ cluster by freezing its total magnetic moment as $14\mu_B$, but the results showed that this isomer is 2.1 eV higher in energy. The average binding energy of the Fe_4 cluster inside the cage is estimated to be 2.24 eV/atom. Thus, it is clear that the stability of the Fe_4 cluster is enhanced inside the cage of $(BN)_{36}$ cluster.

The geometrical structure of the Co_4 tetramer cluster has been investigated by many workers and it has been realized that Co_4 prefers to form a bent rhombus configuration as the ground state structure with total magnetic moment of $10\mu_B$.[47,48] Our calculation also suggest a bent rhombus geometry as the most preferred isomer with all bond lengths of 2.14 Å and a magnetic moment of $10\mu_B$. The dihedral angle of atom 3 from the plane formed by 1-2-4 atoms is 110.93°. The binding energy of this Co_4 cluster is estimated to be 2.27 eV/atom. Another isomer with compact motif (DA =63.64°) and $6\mu_B$ magnetic moment is found to be at 0.8 eV higher in energy.When the geometry of Co_4 was optimized inside the $(BN)_{36}$ cage, significant geometrical changes has been observed. The open rhombus structure bends into a compact tetrahedral geometry as the dihedral angle reduces from 111° to 69°. This structural change is considered to be significant in comparison to other elements. Due to this structural change, the arms (1-2, 1-4, 2-3, and 3-4) are elongated and the diagonal bonds (1-3 and 2-4) are reduced considerably to form the close packed tetrahedral configuration. The smallest Co-B and Co-N distances are 2.18 and 2.32 Å, respectively, which indicate that the smallest Co-B distance is 0.14 Å less than that of Co-N distance. The total magnetic moment of the Co_4 encapsulated inside $(BN)_{36}$ cage is calculated to be $6\mu_B$. The reduction in the magnetic moment is attributed to the structural transition of Co_4 tetramer to a more compact geometry. As stated before, similar bent rhombus structure with DA=63.64° and $6\mu_B$ magnetic moment was found be the second lowest energy structure for the bare cluster. The average binding energy of the Co_4 cluster inside the cage is estimated to be 2.44 eV/atom. The higher stability of the Co_4 cluster inside the cage in comparison to its bare state indicates that it is possible to encapsulate these clusters inside the BN nanocage.

Previous studies on the Ni tetramer cluster showed that it favors tetrahedron configuration as the lowest energy isomer.[48,49] In line with previous results, the present calculations show the distorted tetrahedron as the lowest energy isomer with magnetic moment of $4\mu_B$. The distance between Ni-Ni atoms are found to be 2.31 (1-2, 1-4, 2-3, and 3-4) and 2.21 Å (1-3 and 2-4) and DA=73°. The average binding energy of this Ni_4 cluster is found to be to be 2.26 eV/atom.The optimized geometry of the Ni_4 cluster inside the $(BN)_{36}$ cage suggest negligible change in the geometry in comparison to that of the free state. In particular, the geometry is now opened up slightly as the dihedral angle of atom 3 from the plane of remaining atoms has increased from 73° to 75°. Small bonds (1-2, 1-4, 2-3, and 3-4) were marginally effected by 0.03 Å but the larger diagonal bonds 1-3 and 2-4 were elongated up to 2.44 and 2.35 Å, respectively. However, interestingly, this small change in the geometry of Ni_4 has reduced the magnetic moment from $4\mu_B$ to $2\mu_B$. It may be noted that the T_d isomer with $4\mu_B$ magnetic moment (DA=74°), when optimized inside the cage, shows 1.18 eV higher in energy. For $Ni_4(BN)_{36}$ cluster, the Ni-B and Ni-N distances are found to be 2.17 and 2.22 Å, respectively. It has been noted that in case the optimization of $Ni_4(BN)_{36}$ is carried out by freezing the magnetic moment at $4\mu_B$, the total energy is found to be higher by 1.19 eV. The average binding energy of the Ni_4 cluster inside the cage is estimated to be 2.66 eV/atom, which is 0.40 eV/atom more than its stability outside the cage. Therefore, Ni clusters can be grown inside the cage more efficiently than outside.

The ground state geometry of the Cu_4 cluster has been reported based on density functional,[50–52] hybrid functional,[53] and tight binding[54] calculations. Although the results are different depending on the method adopted, but an overall trend suggests that Cu_4 cluster favors planar square or rhombus structure over three dimensional conformations. In the present work, we found a planar rhombus as the lowest energy isomer (D_{2h}) with zero magnetic moment, which is in line with previous reports. The binding energy of this Cu_4 cluster is estimated to be 1.39 eV/atom. The square planar isomers (D_{4h}) with magnetic moments of $2\mu_B$ and $0\mu_B$ are found to be 0.78 and 0.91 eV higher in energy, respectively. Another isomer, which shows bent rhombus (D_2 symmetry) geometry, is 0.81 eV above in energy. In sharp contrast to this, the optimized geometry of the $Cu_4(BN)_{36}$ cluster shows distorted tetrahedron. Here, it should be noted that although the geometry of Cu_4 is a planar rhombus in the bare state, it relaxed into a close packed geometry inside the $(BN)_{36}$ cluster. This significant deformation in the geometrical configuration results in lower stability of the Cu_4 cluster inside the cage. The diagonal bonds 1-3 and 2-4 have shortened to 2.35 and 2.77 Å, respectively. For the encapsulated $Cu_4(BN)_{36}$ cluster, the Cu-B and Cu-N distances are found to be 2.19 and 2.16 Å, respectively. The average binding energy of the Cu_4 cluster inside the cage is estimated to be 1.21 eV/atom, which is lower than the binding energy of Cu_4 outside the cage.

C. Electronic and magnetic properties of $M_4(BN)_{36}$ clusters

Once the geometrical configurations of M_4 clusters are established, we now discuss the energetics which primarily govern their stability aspects. In Table V, we have listed the binding energy (inside and outside) and interaction energies of M_4 with (BN) cage. While the binding energy provides information about their stability inside and outside the cage, the interaction energy shows the strength of interaction between $(BN)_{36}$ and M_4 cluster inside it. From Table V, it is clear that in all clusters (except Cu), the interaction energy is negative, i.e., magnetic clusters are interacting with cage strongly. A comparison in the binding energy of M_4 clusters inside and outside the cage indicates that while V_4, Fe_4, Co_4, and Ni_4 are more stable inside the cage, Ti_4, Cr_4, Mn_4, and Cu_4 are more stable outside the cage. Such difference in the

TABLE V. Interaction energy (interaction energy (IE) $=E[M_4(BN)_{36}]_{opt}-E[(BN)_{36}]_{opt}-E(M_4)_{having\ inside\ geometry}$) (IE) and binding energy (binding energy (BE)$=E[M_4(BN)_{36}]_{opt}-E[(BN)_{36}]_{opt}-4E(M)$) (BE) of M_4 clusters in encapsulated state. Last column give the total binding energy of M_4 Clusters in free state.

$M_4(BN)_{36}$	μ_B	IE (eV)	BE (eV)	BE (eV) (free M_4)
Ti	2	−0.31	−10.05	−10.41
V	0	−0.51	−9.94	−9.52
Cr	8	−3.79	−3.04	−5.13
Mn	10	−2.68	−4.16	−4.66
Fe	10	−1.12	−8.96	−8.54
Co	6	−1.57	−9.76	−9.10
Ni	2	−1.73	−10.64	−9.04
Cu	0	0.59	−4.84	−6.33

stability of these clusters can be related to the (i) geometrical deformation (ii) strength of M-M, M-B and M-N interactions, (iii) amount of packing of M_4 cluster (value of DA) inside the cage and its comparison with the counterpart of free state, and (iv) the magnetic structure of the M_4 clusters inside and outside the cage. It may be noted that all M_4 clusters that have a compact structure (C_{3v} or T_d, DA$\sim$70°) as the lowest energy isomer in the free state improves their stability inside the $(BN)_{36}$ cage.

In order to illustrate the variation in the magnetic moment of M_4 clusters outside and inside the cage of the $(BN)_{36}$ cluster, we have plotted their total moments, as shown in Fig. 5. In case of bare M_4 clusters, it is found that V_4, Cr_4, and Cu_4 favor singlet spin multiplicity in these series of tetramer clusters. The comparison of these two curves [M_4 and $M_4(BN)_{36}$] shows that in general the total magnetic moment

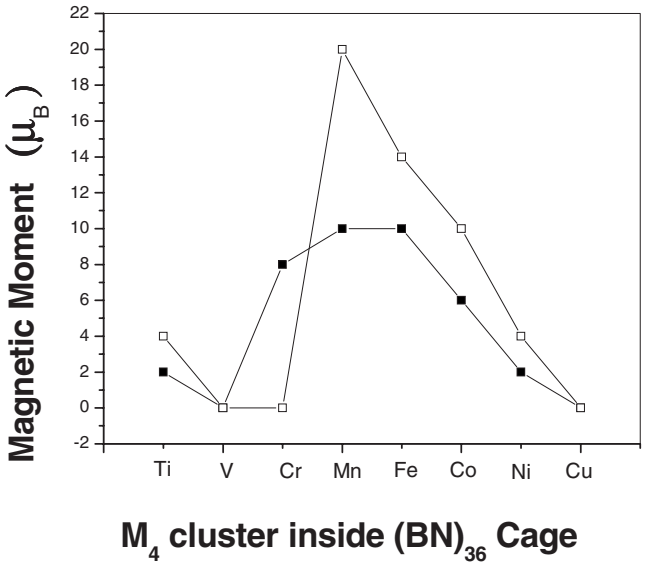

FIG. 5. Comparative magnetic moments (μ_B) of M_4 and $M_4(BN)_{36}$ clusters shown by empty and filled squares, respectively.

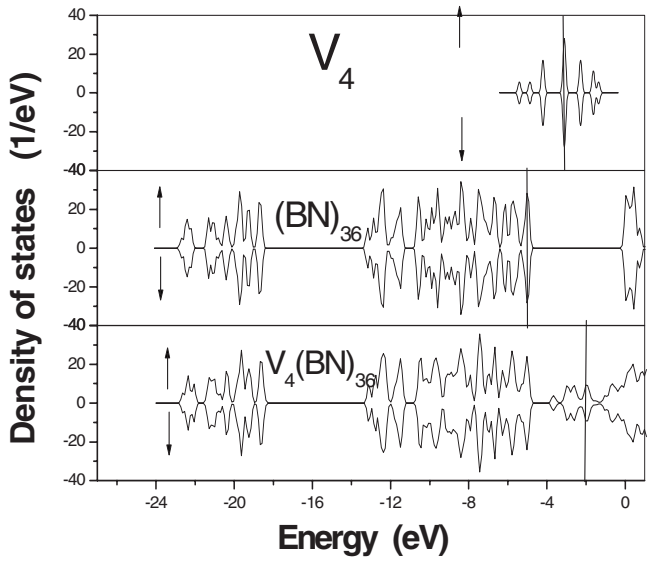

FIG. 6. Density of states of V_4 cluster-free, $(BN)_{36}$ cluster, and $V_4(BN)_{36}$ cluster for up and down spins. The vertical black line represents the HOMO level for up spin for the respective cluster.

of the M_4 clusters are reduced for all the elements except Cr_4, which can be accounted for significant structural modification. The reason for the reduction in the magnetic moment could be explained based on their geometrical changes. For example, in case of open structure, atoms are apart which results in less overlap or more unpaired spin, while in closed structure due to higher overlap of orbital spins may lead to reduction in the total moment.

The detail comparison between the electronic structure of M_4 clusters outside and inside the cage [M_4 vs $M_4(BN)_{36}$] have been studied by plotting their electronic density of states, as presented in Fig. 6. Although we have done the comparison for all systems but for the sake of clarity, we have presented only one typical example of V_4 and $V_4(BN)_{36}$ clusters. From this figure, it is clear that the presence of V_4 cluster in the $(BN)_{36}$ cage has influenced the electronic structure of both V_4 and $(BN)_{36}$ clusters. It is found that the energy state of the V_4 clusters appear in between the large gap (HOMO-LUMO) provided by the $(BN)_{36}$ cage. This trend is followed for all systems studied in this work including the $M(BN)_{36}$ clusters. The appearance of these gap states in the presence of the M_4 clusters results in lowering the HOMO-LUMO gap of these clusters. This implied an induce reactivity of the BN nanocage clusters by the encapsulation of transition metal clusters.

IV. CONCLUSION

Atomic, electronic, and magnetic structures of M and M_4 encaged $(BN)_{36}$ clusters (M=Ti, V, Cr, Mn, Fe, Co, Ni, and Cu) have been investigated under the density functional formalism using the plane-wave based pseudopotential method. For $M(BN)_{36}$, the lowest energy isomers show that the impurity M atom either prefers to stay at the center or placed closed to the periphery by connecting with the hexagonal

ring of the cage. Geometry and electronic structures of M_4 clusters have been optimized inside and outside the octahedral $(BN)_{36}$ cluster. For free M_4 clusters, it is found that depending on the nature of interatomic interactions, they prefer (a) planar rhombus, (b) bent rhombus, and (c) tetrahedral structures. Except Cu_4, which forms a planar rhombus structure, all other tetramer clusters form a three dimensional bent rhombus or tetrahedron. When these M_4 clusters are placed inside the $(BN)_{36}$ cluster cage with different geometrical configurations that have been considered in the free state, the optimized structures of the $M_4(BN)_{36}$ cluster shows significant change in comparison to their free state. The overall trend suggests that all M_4 clusters prefer close packing inside the cage which can be argued to the restrained imposed by the cage diameter. The extent of geometrical changes in the M_4 clusters depends on how open they were outside the cage.

From the energetics point of view, the tetramers of V, Fe, Co, and Ni atoms inside $(BN)_{36}$ were found to enhance their stability, while others such as Ti, Cr, Mn, and Cu tetramers destabilizes inside the $(BN)_{36}$ cage. In general for all M_4 clusters, the magnetic moment values were found to decrease inside the $(BN)_{36}$ cage except that for V_4 and Cu_4. In sharp contrast, for Cr_4, which showed a zero magnetic moment in the bare state, shows $8\mu_B$ when encapsulated inside the $(BN)_{36}$ cage, which is due to the major structural modification. The electronic density of state analysis of $M(BN)_{36}$ and $M_4(BN)_{36}$ clusters shows similar nature, that is, M atoms or M_4 clusters which resides inside the cage introduces energy states in the large energy gap (HOMO-LUMO) originated by the $(BN)_{36}$ octahedral cage. Thus, the BN nanocage can be used to provide a physical coating to the metallic nanoparticles retaining their magnetic character, which may find further application in the magnetoelectronic industries.

ACKNOWLEDGMENT

We are thankful to the members of the computer division, BARC, for their kind cooperation during the work.

*chimaju@barc.gov.in

[1] W. A. de Heer, P. Milani, and A. Chatelain, Phys. Rev. Lett. **65**, 488 (1990); K. Lee, J. Callaway, and S. Dhar, Phys. Rev. B **30**, 1724 (1984).

[2] D. Ma, T. Veres, L. Clime, F. Normandin, J. Guan, D. Kingston, and B. Simard, J. Phys. Chem. C **111**, 1999 (2007); B. Xu, T. Li, P. Han, X. Li, and I. Hideki, Mater. Lett. **60**, 2042 (2006).

[3] N. G. Chopra, R. J. Luyken, K. Herrey, V. H. Crespi, M. L. Cohen, S. G. Louie, and A. Zettl, Science **269**, 966 (1995); X. Blasle, A. Rubio, S. G. Louie, and M. L. Cohen, Europhys. Lett. **28**, 335 (1994); W. Han, Y. Bando, K. Kurashima, and T. Sato, Appl. Phys. Lett. **73**, 3085 (1998); H. J. Xiang, J. Yang, J. G. Hou, and Q. Zhu, Phys. Rev. B **68**, 035427 (2003); F. Banhart, M. Zwanger, and H.-J. Muhr, Chem. Phys. Lett. **231**, 98 (1994); S. Kokado and K. Harigaya, Synth. Met. **135-136**, 745 (2003); D. P. Yu, X. S. Sun, C. S. Lee, I. Bello, S. T. Lee, H. D. Gu, K. M. Leung, G. W. Zhou, Z. F. Dong, and Z. Zhang, Appl. Phys. Lett. **72**, 1966 (1998).

[4] T. Oku, I. Narita, and A. Nishiwaki, Defect Diffus. Forum **113**, 226 (2004).

[5] T. Oku, T. Hirano, M. Kuno, T. Kusunose, K. Niihara, and K. Suganuma, Mater. Sci. Eng., B **74**, 206 (2000).

[6] T. Oku, A. Nishiwaki, I. Narita, and M. Gonda, Chem. Phys. Lett. **380**, 620 (2003).

[7] T. Oku, I. Narita, and A. Nishiwaki, Mater. Manuf. Processes **19**, 1215 (2004).

[8] T. Oku, M. Kuno, H. Kitahara, and I. Narita, Int. J. Inorg. Mater. **3**, 597 (2001).

[9] I. Narita and T. Oku, Solid State Commun. **122**, 465 (2002).

[10] I. Narita and T. Oku, Diamond Relat. Mater. **12**, 1146 (2003); **12**, 1138 (2003).

[11] T. Oku, K. Hiraga, T. Matsuda, T. Hirai, and M. Hirabayashi, Diamond Relat. Mater. **12**, 1138 (2003).

[12] N. Koia, T. Oku, and M. Nishijimab, Solid State Commun. **136**, 342 (2005).

[13] T. Oku, Ichihito Narita, and Hisato Tokoro, J. Phys. Chem. Solids **67**, 1152 (2006).

[14] T. Oku and K. Suganuma, Diamond Relat. Mater. **10**, 1205 (2001); T. Oku, M. Kuno, and I. Narita, *ibid.* **11**, 945 (2002); T. Oku, I. Narita, and A. Nishiwaki, J. Phys. Chem. Solids **65**, 369 (2004); A. Nishiwaki, T. Oku, and K. Suganuma, Physica B **349**, 254 (2004).

[15] N. Koi and T. Oku, Solid State Commun. **131**, 121 (2004); T. Oku and I. Narita, Physica B **323**, 216 (2002).

[16] O. Stephan, Y. Bando, A. Loiseau, F. Willaime, N. Shramchenko, T. Tamiya, and T. Sato, Appl. Phys. A: Mater. Sci. Process. **67**, 107 (1998).

[17] D. Golberg, Y. Bando, O. Stephan, and K. Kurashima, Appl. Phys. Lett. **73**, 2441 (1998); D. Golberg, Y. Bando, K. Kurashima, and T. Sasaki, *ibid.* **72**, 2108 (1998); D. Golberg, W. Han, Y. Bando, L. Bourgeois, K. Kurashima, and T. Sato, J. Appl. Phys. **86**, 2364 (1999).

[18] S. S. Alexandre, M. S. C. Mazzoni, and H. Chacham, Appl. Phys. Lett. **75**, 61 (1999); S. S. Alexandre, R. W. Nunes, and H. Chacham, Phys. Rev. B **66**, 085406 (2002).

[19] M. Terauchi, M. Tanaka, H. Matsada, M. Takeda, and K. Kimura, J. Electron Microsc. **46**, 75 (1997).

[20] Y. Bando, K. Ogawa, and D. Golgerg, Chem. Phys. Lett. **347**, 349 (2001).

[21] C. Tang, Y. Bando, D. Golberg, X. Ding, and S. Qi, J. Phys. Chem. B **107**, 6539 (2003).

[22] Wei-Qiang Han, C. W. Chang, and A. Zettl, Nano Lett. **4**, 1355 (2004).

[23] F. Xu, Y. Bando, D. Golberg, M. Hasegawa, and M. Mitome, Acta Mater. **52**, 601 (2004).

[24] G. W. Peng, A. C. H. Huan, and Y. P. Feng, Appl. Phys. Lett. **88**, 193117 (2006).

[25] R. J. C. Batista, M. S. C. Mazzoni, and H. Chacham, Phys. Rev. B **75**, 035417 (2007).

[26] G. Kresse and J. Furthmuller, Phys. Rev. B **54**, 11169 (1996);

Comput. Mater. Sci. **6**, 15 (1996); D. Vanderbilt, Phys. Rev. B **41**, 7892 (1990).
[27] P. E. Blöchl, Phys. Rev. B **50**, 17953 (1994).
[28] G. Kresse and D. Joubert, Phys. Rev. B **59**, 1758 (1999).
[29] J. P. Perdew, K. Burke, and M. Ernzerhof, Phys. Rev. Lett. **77**, 3865 (1996).
[30] P. H. Dederichs, S. Blugel, R. Zeller, and H. Akai, Phys. Rev. Lett. **53**, 2512 (1984); P. Mohn and K. Schwarz, J. Phys. F: Met. Phys. **14**, L129 (1984).
[31] Rajendra R. Zope and Brett I. Dunlap, Chem. Phys. Lett. **386**, 403 (2004).
[32] Q. Sun, Q. Wang, and P. Jena, Nano Lett. **5**, 1273 (2005).
[33] C. J. Barden, J. C. Rienstra-Kiracofe, and H. F. Schaefer III, J. Chem. Phys. **113**, 690 (2000).
[34] C. Kittel *Introduction to Solid State Physics*, 4th ed. (Wiley, New York, 1971).
[35] S. H. Wei, Zhi Zeng, J. Q. You, X. H. Yan, and X. G. Gong, J. Chem. Phys. **113**, 11127 (2000).
[36] J. Zhao, Q. Qiu, B. Wang, J. Wang, and G. Wang, Solid State Commun. **118**, 157 (2001).
[37] M. Castro, S. Liu, H. Zhai, and Lai-Sheng Wang, J. Chem. Phys. **118**, 2116 (2003).
[38] Henrik Gronbeck and Arne Rosen, J. Chem. Phys. **107**, 10620 (1997).
[39] X. Wu and A. K. Ray, J. Chem. Phys. **110**, 2437 (1999).
[40] S. Li, M. M. G. Alemany, and J. R. Chelikowsky, J. Chem. Phys. **121**, 5893 (2004).
[41] H. Cheng and Lai-Sheng Wang, Phys. Rev. Lett. **77**, 51 (1996).
[42] D. Hobbs, G. Kresse, and J. Hafner, Phys. Rev. B **62**, 11556 (2000).
[43] Q. Wang, Q. Sun, B. K. Rao, P. Jena, and Y. Kawazoe, J. Chem. Phys. **119**, 7124 (2003).
[44] M. R. Pederson, F. Reuse, and S. N. Khanna, Phys. Rev. B **58**, 5632 (1998).
[45] P. Bobadova-Parvanova, K. A. Jackson, S. Srinivas, and M. Horoi, J. Chem. Phys. **122**, 014310 (2005).
[46] J. L. Chen, C. S. Wang, K. A. Jackson, and M. R. Pederson, Phys. Rev. B **44**, 6558 (1991).
[47] N. O. Jones, M. R. Beltran, S. N. Khanna, T. Baruah, and M. R. Pederson, Phys. Rev. B **70**, 165406 (2004).
[48] L. Giordano, G. Pacchioni, A. M. Ferrari, F. Illas, and N. Rosch, Surf. Sci. **473**, 213 (2001).
[49] E. Curotto, Alexander Matro, David L. Freeman, and J. D. Doll, J. Chem. Phys. **108**, 729 (1997).
[50] P. Calaminici, A. M. Koster, N. Russo, and D. R. Salahub, J. Chem. Phys. **105**, 9546 (1996).
[51] K. Jug, B. Zimmermann, P. Calaminici, and A. M. Koster, J. Chem. Phys. **116**, 4497 (2002).
[52] S. Li, M. M. G. Alemany, and J. R. Chelikowsky, J. Chem. Phys. **125**, 034311 (2006).
[53] Pablo Jaque and Alejandro Toro-Labbé, J. Chem. Phys. **117**, 3208 (2002).
[54] M. Kabir, A. Mookerjee, and A. K. Bhattacharya, Phys. Rev. A **69**, 043203 (2004).